Applied Geochemistry 140 (2022) 105297

Contents lists available at ScienceDirect

Applied Geochemistry

journal homepage: www.elsevier.com/locate/apgeochem

The impact of phosphate on the interaction of Sb(III) with ferrous sulfide

Qingyun Wang [a,b], Guoping Zhang [a,*], Shirong Liu [a], Kuan Mao [a,b], Chao Ma [a], Jingjing Chen [a], Fengjuan Liu [c]

[a] State Key Laboratory of Environmental Geochemistry, Institute of Geochemistry, Chinese Academy of Sciences, Guiyang, 550081, China
[b] University of Chinese Academy of Sciences, Beijing, 100049, China
[c] School of Geography and Tourism, Guizhou Education University, Guiyang, 550018, China

ARTICLE INFO

Editorial handling by Jon Petter Gustafsson

Keywords:
FeS
Antimony
Interaction
Phosphate
Impact

ABSTRACT

Phosphate may affect the behavior of metal(loid)s in environments, so the interaction of Sb(III) with FeS affected by phosphate was investigated in this study. Sb(III) was reacted with synthesized FeS in solution at pH 5.5, 7.0, and 9.0 with and without the addition of phosphate. The concentrations of Fe(II), Sb(III), and phosphate in the solution were monitored, and the solid phases were examined by XRD, TEM, and XPS. For the interaction of Sb (III) with FeS in the absence of phosphate, the formation of Sb_2S_3 was very important at pH 5.5 and 7.0, whereas Sb(III) adsorption was the dominant process at pH 9.0. The interaction of Sb(III) with FeS could be significantly affected by phosphate, and this impact was dependent of pH and phosphate concentration. At pH 5.5 and 7.0, the effect of phosphate varied markedly with increasing phosphate concentration. Low phosphate loadings (9.5 and 19 mg/L) had a negligible effect on the mobility of Sb(III), while high phosphate loadings (95 and 475 mg/L) notably enhanced the uptake of Sb(III) by FeS. In the case of high phosphate loadings, $Fe_3(PO_4)_2{\cdot}8H_2O$ was formed and resulted in the dissolution of FeS, which was favorable for the formation of Sb_2S_3 and consequently the uptake of Sb(III). In the experiments at pH 9.0, the addition of phosphate only resulted in minor desorption of Sb(III) because FeS was very stable and consequently both $Fe_3(PO_4)_2{\cdot}8H_2O$ and Sb_2S_3 were unlikely to be formed. The results of this work may help to better understand the effect of phosphate on the behavior of Sb in some anoxic environments where FeS is present.

1. Introduction

Antimony is a toxic and carcinogenic metalloid of global concern (Amarasiriwardena and Wu, 2011; Kulp et al., 2014). It has been recognized as a pollutant of priority interest by the European Union and the United States Environmental Protection Agency (Ungureanu et al., 2015). The release of Sb into the environment can occur as a result of human activities related to mining and some industrial processes such as mining/smelting and the manufacture of alloys, semiconductors, fire retardants, glass, and polyethylene terephthalate (Filella et al., 2002a; He et al., 2012). In environmental systems, Sb can be present in four oxidation states (−3, 0, +3, and +5) but is mostly found in two oxidation states (+3 and + 5). It usually occurs as $Sb(OH)_6^-$ (Sb(V)) in relatively oxic environments or $Sb(OH)_3$ (Sb(III)) in anoxic environments (Filella et al., 2002a, 2002b; Wilson et al., 2010). In sulfidic systems, Sb can react with sulfide and lead to the formation of thioantimonite complexes such as $HSb_2S_4^-$ or $Sb_2S_4^-$ (Spycher and Reed, 1989; Polack et al., 2009; Hockmann et al., 2020).

The mobility of metal(loid)s in the environment has been recognized to be highly related to minerals. In terrestrial environments, ubiquitous Fe(III) hydro(oxides) such as ferrihydrite, goethite, and hematite are recognized as the primary host phases for metal(loid)s. In anoxic environments, however, reductive transformation of Fe(III) hydro(oxides) occurs due to microorganisms or reducing agents and metal(loid)s are subsequently released and redistributed (Li et al., 2006; Kocar et al., 2010; Burton et al., 2011). Meanwhile, sulfate-reducing bacteria in anoxic environments can reduce sulfate to sulfide that subsequently reacts with ferrous ion (Watson et al., 1995; Jong and Parry, 2003). Amorphous FeS is typically the initial iron sulfide phase to be formed post to the reduction of Fe(III) hydro(oxides). It is generally considered a nanocrystalline form of mackinawite (Wolthers et al., 2003; Burton et al., 2011, 2019). The newly formed FeS can serve as a major sink of metal(loid)s that are released from the reductive transformation of Fe (III) hydro(oxides). For example, As(III) and Sb(III) have been

* Corresponding author.
E-mail address: zhangguoping@vip.gyig.ac.cn (G. Zhang).

https://doi.org/10.1016/j.apgeochem.2022.105297
Received 18 January 2022; Received in revised form 2 April 2022; Accepted 5 April 2022
Available online 9 April 2022

recognized to be significantly sequestered by FeS in anoxic environments (Han et al., 2011, 2018). As a consequence, FeS can significantly affect the mobility of metal(loid)s in sediment or groundwater (Wolthers et al., 2003, 2005; Han et al., 2011).

Increased inputs of nutrients into rivers, lakes, and estuaries can affect the mobility of metal(loid)s in supergene environments (Park et al., 2018; Neidhardt et al., 2021). For example, dissolved As can entirely adsorb to aquifer sediments in the absence of PO_4^{3-}, whereas strong competition between PO_4^{3-} and dissolved inorganic As in the form of AsO_3^{3-} and AsO_4^{3-} can be assumed when PO_4^{3-} is present (Biswas et al., 2014; von Bromssen et al., 2008). Competition of PO_4^{3-} and As for sorption sites was observed by Rathi et al. (2017) in laboratory sorption experiments using orange-colored aquifer sediment. As a result of the competition between PO_4^{3-} and As, remarkably high PO_4^{3-} and As concentrations were observed in anoxic groundwater of floodplain aquifers in large Asian deltas such as the Bengal Delta or the Red River Delta (Neidhardt et al., 2018; Podgorski and Berg, 2020).

In the interaction with FeS under anoxic conditions, As(III) or Sb(III) can react strongly with FeS. Previous studies reported the formation of As(III)–S complex or As_2S_3 (Wolthers et al., 2005; Han et al., 2011, 2018; Burton et al., 2014), AsS (Han et al., 2011), Sb(III)–S complex or Sb_2S_3 (Han et al., 2018; Li et al., 2021) or SbS_3-like precipitates (Kirsch et al., 2008) on the surface of FeS. The interaction between metal(loid)s and FeS particles may become more complicated in the presence of PO_4^{3-}. Particularly, co-existence of $Fe_3(PO_4)_2{\cdot}8H_2O$ and FeS was observed in the biotic transformation of schwertmannite coupled with PO_4^{3-} addition (Schoepfer et al., 2019) and at the sediment-water interface of an urban canal (Dodd et al., 2003). Moreover, in the application of phosphate to the mitigation of metal(loid) mobility (Munksgaard and Lottermoser, 2013; Saavedra-Mella et al., 2019) in some sulfidic mine tailings, high concentrations of PO_4^{3-} and Sb can be present in anoxic layers where reduction of abundant sulfate and Fe(III) to H_2S and Fe(II) can also occur. The crystalline precipitate of $Fe_3(PO_4)_2{\cdot}8H_2O$ is called vivanite, which is an authigenic mineral that is commonly found in aquatic systems, terrestrial systems as well as wastewater sludges (Rothe et al., 2016). As to the effect of PO_4^{3-} on the interaction of As(III) with FeS, Niazi and Burton (2016) reported that PO_4^{3-} had a negligible effect on the sorption of As(III) on FeS in the pH range of 6–9. Park et al. (2018) added oxidized and fresh FeS into metal(loid)-contaminated soil and investigated the mobility of As and Sb under oxic and anoxic conditions, and concluded that the presence of PO_4^{3-} apparently inhibited the sorption of As but did not significantly change Sb sorption. We hypothesized that the interaction of Sb(III) with FeS may be affect by PO_4^{3-} via the formation of $Fe_3(PO_4)_2{\cdot}8H_2O$. To examine this hypothesis, we reacted aqueous Sb(III) with synthesized FeS under anoxic conditions (in the absence and presence of PO_4^{3-}) and monitored the mobility of Sb in this system, so as to better understand the mobility of Sb in anoxic environments that received high inputs of PO_4^{3-}.

2. Materials and methods

2.1. Materials

Deionized water (DW) (resistivity: 18.2 MΩ cm) was prepared with a Milli-Q system (Millipore, Bedford, MA, USA). Deoxygenated deionized water (DDW) was prepared by sparging DW with high-purity N_2 (99.99%). Potassium antimonyl tartrate (PAT) sesquihydrate (>99% purity) was purchased from Acros Organics Inc. (New Jersey, USA). Ferrous sulfate heptahydrate ($FeSO_4{\cdot}7H_2O$), sodium sulfide nonahydrate ($Na_2S{\cdot}9H_2O$), anhydrous dibasic sodium phosphate (Na_2HPO_4), and other chemicals were of analytical grade. All solutions were prepared with DDW. Stock solutions of Sb(III) (500 mg/L), S(–II) (6.4 g/L, 0.2 M), and Fe(II) (11.2 g/L, 0.2 M) were prepared by dissolving potassium antimonyl tartrate sesquihydrate, sodium sulfide nonahydrate, and ferrous sulfate heptahydrate in DDW, respectively.

The use of PAT as a source of Sb(III) has been criticized due to the possible complexation of Sb(III) by tartrate (Filella and Williams, 2010; Filella and Williams, 2012). However, Li et al. (2019) reported that the effect of 0.5 mM tartrate on the adsorption of Sb(III) on granular ferric hydroxide was likely minor. Moreover, the high solubility of PAT allowed the use of high Sb(III) concentrations (20 mg/L) in our experiments, while the solubility of another frequently used Sb(III) reagent - Sb_2O_3 was reported to be only 12.6 mg (Sb)/L (Gayer and Garrett, 1952).

2.2. Synthesis of FeS and experiments

The synthesis of FeS and the interaction of Sb(III) with FeS in the absence and presence of PO_4^{3-} were conducted in an anaerobic chamber (Model 855-ACB, PLAS-LABS, CO, USA) at an atmospheric composition of 95% Ar/5% H_2. The residual oxygen inside the chamber was removed by Pd catalysts, resulting in an oxygen concentration below 1 ppm.

For the synthesis of FeS, a method proposed by Jeong et al. (2008) was applied. In brief, 0.2 M $FeSO_4$ solution and 0.2 M Na_2S solution (V:V = 1:1) were mixed and black FeS precipitates were quickly formed. The characteristics of FeS synthesized by the reaction of Fe(II) with S(–II) were previously reported by Ma et al. (2020) and Li et al. (2021). The XRD pattern of the FeS precipitates is shown in Fig. 1. Overall, the synthesized FeS was amorphous and appeared as clusters of very fine grains because FeS particles tended to agglomerate rapidly.

The freshly precipitated FeS was aged for 3 h before it was used for the experiments on the interaction of Sb(III) with FeS. Sodium chloride was added to obtain 0.1 M (5.85 g/L) NaCl as a background ionic medium. Then, stock solutions of Sb(III) and PO_4^{3-} were added into the FeS suspension to obtain preset initial Sb(III) and PO_4^{3-} concentrations. The pH of the initial suspension was adjusted by the addition of 0.1 M HCl and 0.1 M NaOH. The initial volume of the solution was adjusted to 50 mL through the addition of DDW. The reaction mixture was sampled at the end of experiments. After collection, the solution sample was immediately filtered using a cellulose membrane (0.22 μm pore size) for determination of the pH and the concentrations of dissolved Sb(III), Fe (II), and PO_4^{3-}. The final solid phases of the experiments were separated and immediately dried using a vacuum freeze drier.

Batch experiments on the interaction of Sb(III) with FeS in the absence and presence of PO_4^{3-} were carried out. For all experiments, the initial concentrations of FeS and Sb(III) were preset to 44 mg/L and 20 mg/L, respectively. After mixing of FeS particles and Sb(III) solution, PO_4^{3-} solution was added. In the experiments in the presence of PO_4^{3-},

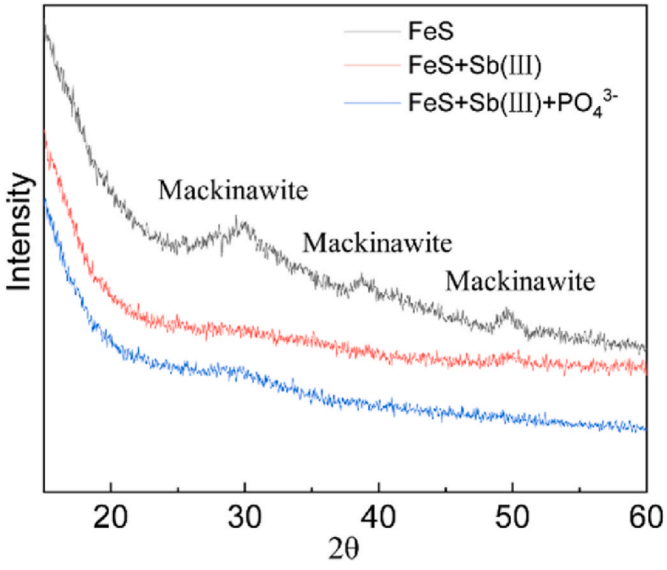

Fig. 1. The XRD patterns of the synthesized FeS and the solid phases of experiments P-0 and P-95.

the initial concentration of PO_4^{3-} was preset at low loadings (9.5 and 19 mg/L) and high loadings (95 and 475 mg/L). Experiments were conducted in polyethylene vials. The vials were removed from the anaerobic chamber and placed on a shaker to mix the suspensions thoroughly. The reaction time was 24 h. All experiments were carried out at room temperature (20–25 °C) in triplicate. Other details for each experiment were later given in the caption of the figures.

2.3. Analyses and solid characterization

The pH of the solution was measured with a Denver UB-7 pH-meter. The concentration of Fe(II) was measured by a 1,10-phenanthroline spectrophotometric method (APHA, 1998). The precision of the measurement of Fe(II) in the solution was better than 3%. Dissolved sulfide was measured immediately using the methylene blue method (Greenberg et al., 1992) (detection limit: 0.2 mg/L). The concentration of PO_4^{3-} was determined by an ammonium molybdate spectrometric method (Liu et al., 2021), and the concentration of Sb(III) was determined by hydride generation-atomic fluorescence spectrometry (HG-AFS) (AFS-2202E, Haiguang Instruments Corp., Beijing, China) following a method from Fu et al. (2016). The limit of detection for Sb (III) based on 11 replicate analyses was 0.05 μg/L, and the relative standard deviation was 0.6%.

The mineralogy of the synthesized FeS and the solid phases after interaction was characterized by X-ray diffractometer (Empyrean, PANanalytical Co., The Netherlands) using a Cu tube and a scanning range from 4° to 60° with a step size of 0.03° and 8 s/step measuring time. The solid phases after the interaction were also examined by a field emission transmission electron microscope equipped with an energy dispersive spectrometer (TEM-EDS, Tecnai G2 F20 S-TWIN, FEI Inc., USA) and X-ray photoelectron spectroscopy (XPS, ESCALAB 250Xi, Thermo Fisher Scientific, Inc, USA).

3. Results and discussion

3.1. The FeS + Sb(III) system

For the experiments at pH 5.5, 7.0, and 9.0, the concentrations of Sb $(III)_{aq}$ after the interaction of Sb(III) with FeS were 6.9, 9.6, and 13.8 mg/L, respectively (Fig. 2, experiment P-0). The lower $Sb(III)_{aq}$ concentration at lower pH indicated that the uptake of Sb(III) increased with decreasing pH. Meanwhile, the concentration of $Fe(II)_{aq}$ increased notably with decreasing pH (Fig. 2b, experiments P-0), indicating that the dissolution of FeS greatly increased with decreasing pH. Consistently, the higher dissolution of FeS at lower pH has also been previously reported (Wolthers et al., 2005; Han et al., 2018; Li et al., 2021). In detail, the corresponding concentrations of solid FeS after interaction at pH 5.5, 7.0, and 9.0 were 15.3, 40.8, and 43.9 mg/L, respectively. Overall, the pH 5.5 experiments showed the highest uptake of Sb(III) while it had the least solid FeS, implying that an important mechanism have notably increased the uptake of Sb(III) at low pH.

For the experiments at pH 5.5 and 7.0, the TEM-EDS analysis of the solid phases showed strong signals of Sb and S (Fig. 3), so precipitation of Sb_2S_3 was suggested to be important for the uptake of Sb(III) by FeS under acidic and neutral conditions. This notion was in agreement with that of previous studies (Han et al., 2018; Li et al., 2021). It should be noted that electrostatic adsorption and Sb(III)–S surface complexes could also contribute to the uptake of Sb(III). In previous studies, the formation of SbS_3-like solid (Kirsch et al., 2008) and surface complex Sb–S (Han et al., 2018) has been proposed. For the pH 9.0 experiments, Sb_2S_3 was not been found in the solid phases. A typical result of the TEM-EDS examination of all the pH 9.0 samples is shown in Fig. S1. It was proposed that Sb(III) was primarily sequestered by FeS through adsorption. The adsorption of Sb(III) at pH 9.0 could be related to the species of $Sb(OH)_3$ and $Sb(OH)_4^-$. Han et al. (2020) reported that As could be bound to FeS on the Fe(II) and S(–II) sites. Moreover, in a study

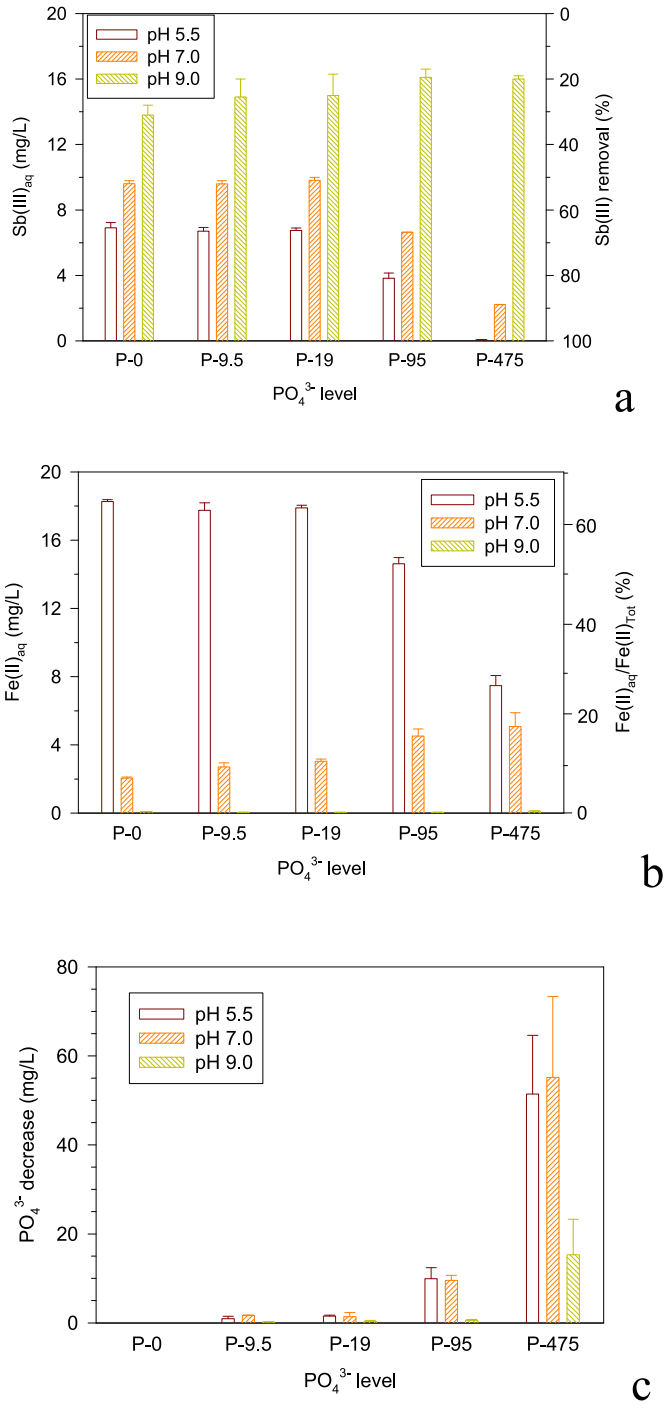

Fig. 2. Aqueous Sb(III), Fe(II), and PO_4^{3-} concentrations of the experiments (P-0, P-9.5, P-19, P-95, and P-475 represent the experiments in the presence of 0, 9.5, 19, 95, and 475 mg/L phosphate, respectively).

on the adsorption of As(III) on FeS particles, Gallegos et al. (2007) suggested that more As(III) was bound on the Fe(II) sites with increasing pH whereas more As(III) was bound on the S(–II) sites with decreasing pH. Because Sb usually shows a similar chemical behavior to As (Filella et al., 2002a), it is proposed that Sb(III) was primarily bound on the S (–II) sites at pH 5.5 and 7.0 and bound on the Fe(II) sites at pH 9.0.

3.2. The FeS + Sb(III) + PO_4^{3-} system

The concentrations of Sb(III)aq and Fe(II)aq in the FeS + Sb(III) + PO_4^{3-} experiments are also shown in Fig. 2 for comparison with the FeS

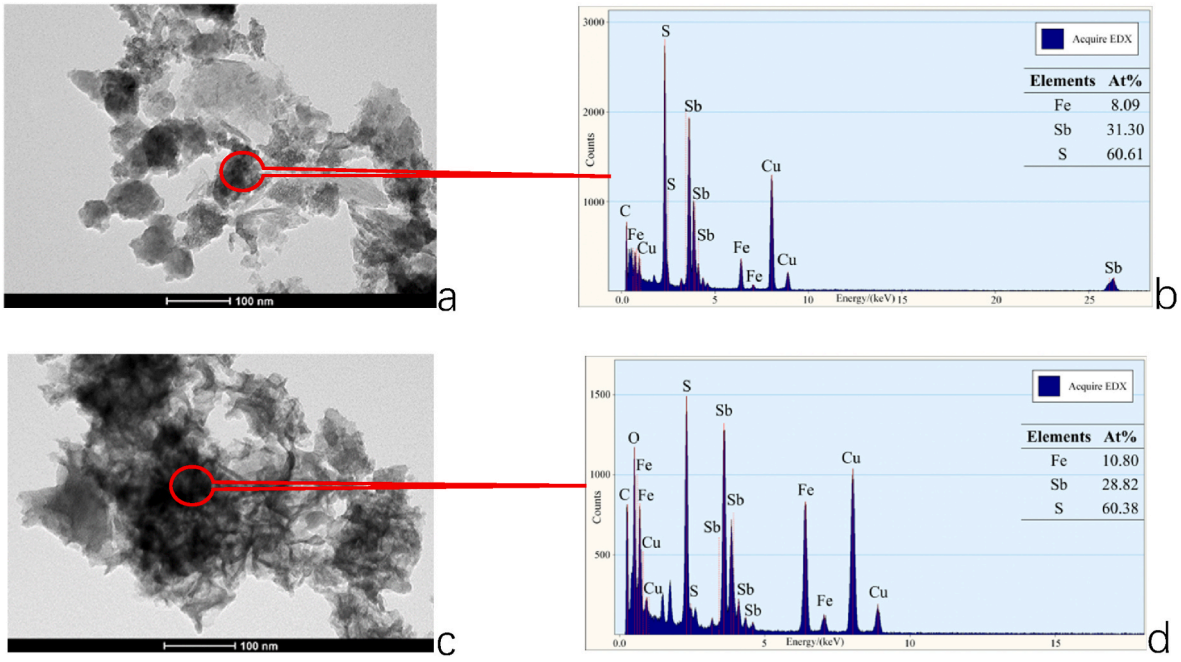

Fig. 3. Precipitates of Sb_2S_3 in the solid phases of experiments P-0 (a and b: TEM image and EDS spectrum of pH 5.5 sample; c and d: TEM image and EDS spectrum of pH 7.0 sample) (The signal of Cu, C, and O originated from the support grids for sample).

+ Sb(III) experiments. P-9.5 and P-19 represent the experiments with low PO_4^{3-} loadings (9.5 and 19 mg/L), while P-95 and P-475 represent the experiments with high PO_4^{3-} loadings (95 and 475 mg/L).

For the FeS + Sb(III) + PO_4^{3-} experiments at pH 5.5 and 7.0, the effect of high PO_4^{3-} loadings differed significantly from that of low PO_4^{3-} loadings. The concentration of $Sb(III)_{aq}$ did not vary when the concentration of PO_4^{3-} increased from 0 to 19 mg/L, but decreased significantly when the concentration of PO_4^{3-} increased to 95 and 475 mg/L (Fig. 2a). This indicated that, at pH 5.5 and 7.0, low PO_4^{3-} loadings had a negligible effect on the uptake of Sb(III) but high PO_4^{3-} loadings notably enhanced the uptake of Sb(III). Moreover, in the TEM-EDS examination of the solid phases, $Fe_3(PO_4)_2{\cdot}8H_2O$ and Sb_2S_3 precipitates were found in experiments P-95 (Fig. 4) and P-475 (Fig. S2), whereas only Sb_2S_3 precipitates were found in experiments P-9.5 and P-19. Overall, for the experiments with high PO_4^{3-} loadings, the occurrence of $Fe_3(PO_4)_2{\cdot}8H_2O$ in the solid phases and the notable decrease in the concentration of $Sb(III)_{aq}$ (Fig. 2a) probably indicated that high PO_4^{3-} loading resulted in the formation of $Fe_3(PO_4)_2{\cdot}8H_2O$ and consequently enhanced the immobilization of Sb(III). The precipitates of $Fe_3(PO_4)_2{\cdot}8H_2O$ and Sb_2S_3 were not discernible in the XRD analysis (Fig. 1), implying that they were amorphous or poorly crystalline. Consistent with the formation of $Fe_3(PO4)_2{\cdot}8H_2O$, the concentration of Fe(II)aq in the pH 5.5 experiments notably decreased when the PO_4^{3-} loading increased to 95 and 475 mg/L (Fig. 2b). However, the concentration of Fe(II)aq in the pH 7.0 experiments gradually increased when PO_4^{3-} loading increased from 0 to 475 mg/L. This result can not be well explained. The precipitation of Sb_2S_3 and $Fe_3(PO4)_2{\cdot}8H_2O$ is specifically discussed in section 3.4.

For the FeS + Sb(III) + PO_4^{3-} experiments at pH 9.0, Sb_2S_3 or $Fe_3(PO4)_2{\cdot}8H_2O$ was not found in TEM-EDS examination of the solid phases (Fig. S1). The concentrations of $Sb(III)_{aq}$ in experiments P-0, P-9.5, P-19, P-95, and P-475 were 13.8, 14.9, 15.0, 16.1, and 16.0 mg/L, respectively (Fig. 2a). The increase in PO_4^{3-} concentration from 0 to 95 mg/L resulted in gradual release of Sb(III) into solution. Meanwhile, the concentrations of $Fe(II)_{aq}$ in these experiments were below 0.1 mg/L (Fig. 2b) and the decrease in the concentrations of PO_4^{3-} in the experiments P-9.5, P-19, and P-95 at pH 9.0 was only 0.17–0.56 mg/L (Fig. 2c), indicating that FeS was stable and PO_4^{3-} adsorption was minor. The effect of PO_4^{3-} on the adsorption of As by FeS was reported to be negligible because As(III) was mostly present as As(III)–S(–II)–like species and this binding mechanism was specific to As(III) (Niazi and Burton, 2016; Han et al., 2020). Similar to As(III), the majority of Sb(III) bound to FeS is suggested to be stable when affected by PO_4^{3-}. Therefore, the small amount of Sb(III) released from solid FeS was likely related to the change of ionic strength.

3.3. XPS spectra of the solid phases after interaction

The XPS Sb-3d spectra of the solid phase samples of the FeS + Sb(III) and FeS + Sb(III) + PO_4^{3-} experiments (P-0 and P-95) are shown in Fig. 5. The signal of Sb(III)–O is considered an indication of Sb(III) species of $Sb(OH)_3$, $Sb(OH)_4^-$, or $Sb(OH)_2^+$ that were electrostatically adsorbed on the surface of FeS or bound to FeS on the sites of Fe(II) or S(–II), whereas the signal of Sb(III)–S is considered an indication of precipitates of Sb_2S_3 or Sb(III) species binding on the S(–II) sites of FeS.

The occurrence of Sb(III) as Sb(III)–S or Sb(III)–O was found to be closely related to pH. The chemical bond of Sb(III)–S was observed in the solid phases of experiments P-0 and P-95 at pH 5.5 and 7.0 (Fig. 5a and b, d, and e), indicating that the formation of Sb_2S_3 or the binding of Sb(III) on the S(–II) sites of FeS was important under acidic or neutral conditions. Moreover, the Sb(III)–S signal of the pH 5.5 sample was stronger than that of the pH 7.0 sample for experiments P-0 (Fig. 5a and b) and P-95 (Fig. 5d and e), indicating that the binding of Sb(III) to S(–II) was more important at lower pH. This result is consistent with the abovementioned notion that Sb_2S_3 formation can be enhanced at lower pH. Additionally, it has been previously reported that Sb(III) was much more importantly bound to FeS on the sites of S(–II) at lower pH (Han et al., 2018; Li et al., 2021). This trend of Sb(III) binding to FeS with respect to pH agrees well with that of As(III). Previous studies reported that more As could be bound to FeS on S(–II) sites with decreasing pH (Gallegos et al., 2007), and the formation of As_2S_3 can be enhanced at lower pH (Wilkin and Ford, 2002; Rodriguez-Freire et al., 2014).

For the pH 9.0 samples of experiments P-0 and P-95, the Sb(III)–O signal was observed (Fig. 5, c and f), whereas the Sb(III)–S signal was absent. This is in good agreement with the above result that adsorption was the dominant process responsible for the uptake of Sb(III) by FeS at

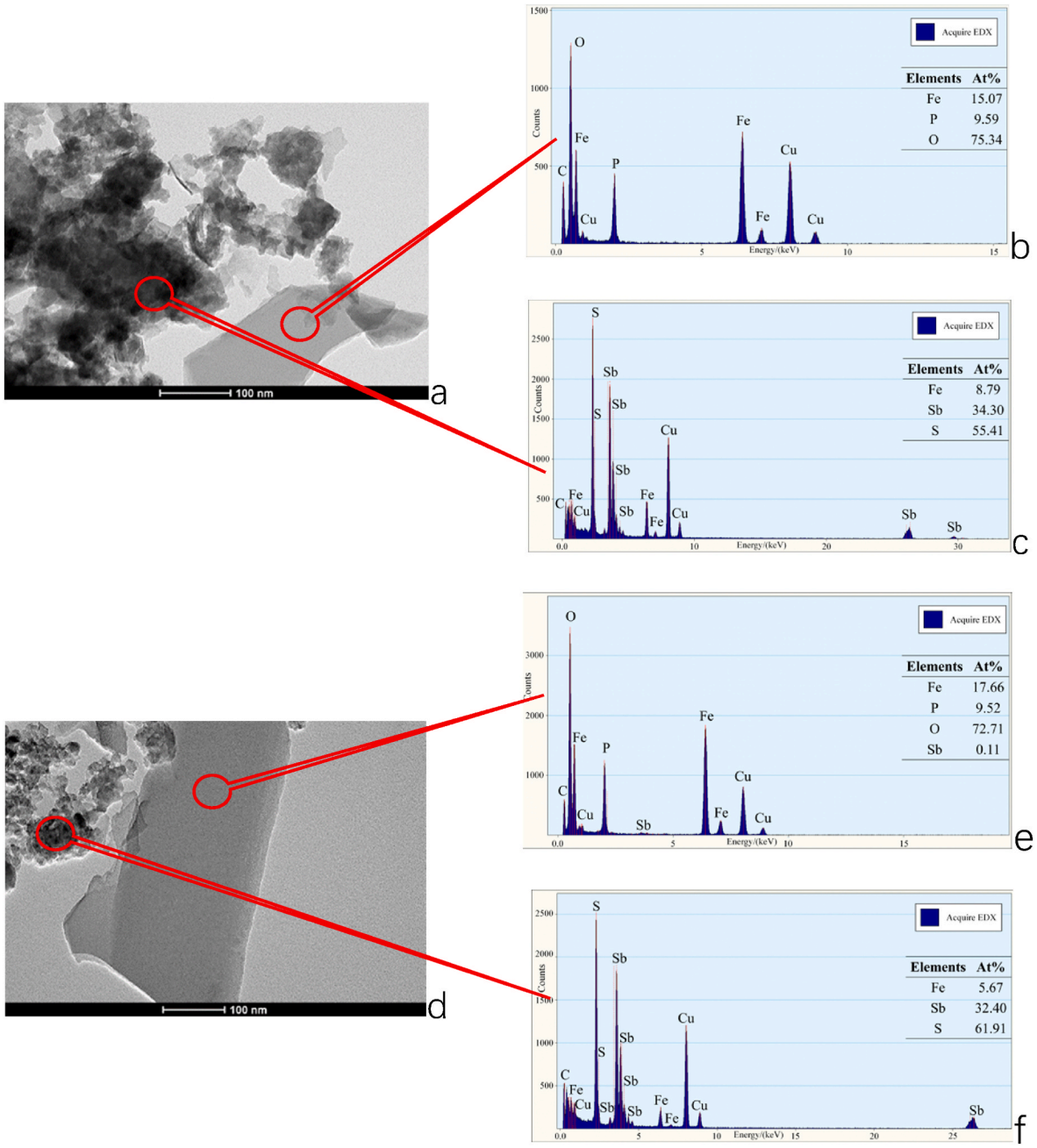

Fig. 4. Precipitates of $Fe_3(PO_4)_2{\cdot}8H_2O$ and Sb_2S_3 in the solid phases of experiments P-95 (a, b, and c: TEM image and EDS spectra of pH 5.5 sample; d, e, and f: TEM image and EDS spectra of pH 7.0 sample) (The signal of Cu, C, and O originated from the support grids for sample).

pH 9.0. The lack of a Sb(III)-S signal supported the notion that precipitation of Sb_2S_3 was not possible at pH 9.0 regardless of whether PO_4^{3-} was present.

The binding of Sb(III) to S(–II) in the solid phases could be significantly affected by high PO_4^{3-} loading. The Sb(III)–S peak of the solid phases of experiment P-95 was stronger than that of experiment P-0 regarding the experiments at pH 5.5 (Fig. 5, a and d) or 7.0 (Fig. 5, b and e), indicating that the presence of high PO_4^{3-} loading (95 mg/L) enhanced the binding of Sb(III) to S(–II). This is consistent with the above result that high PO_4^{3-} loadings enhanced the formation of Sb_2S_3 at pH 5.5 and 7.0. Particularly, for the experiments P-95 at pH 5.5, the signal of the Sb(III)–S bond was strong, whereas the signal of Sb(III)–O was absent (Fig. 5d). This implies that, in the presence of high PO_4^{3-} loadings, most Sb(III) was likely present as Sb_2S_3 precipitates whereas Sb(III) adsorption on FeS was not significant.

For the pH 9.0 samples, the binding of Sb(III)–O can also be affected by PO_4^{3-}. The smaller Sb(III)–O peak of the solid phases of experiment P-95 (Fig. 5f) than that of experiment P-0 (Fig. 5c) possibly reflected the desorption of Sb(III) resulting from the presence of PO_4^{3-}. As described above, the release of Sb(III) into solution gradually increased when the concentration of PO_4^{3-} increased to 95 mg/L.

3.4. Precipitation of Sb_2S_3 and $Fe_3(PO_4)_2{\cdot}8H_2O$

For the interaction of Sb(III) with FeS at pH 5.5 and 7.0, the precipitation of Sb_2S_3 can be attributed to the competition between Sb(III) and Fe(II) for binding to sulfide (Han et al., 2018; Li et al., 2021). The dissolution or precipitation of a compound is dependent of its solubility product (K_{sp}). The solubility product of Sb_2S_3 (Log K_{sp} = −92.8, Mane and Lokhande, 2003) is much lower than that of FeS (Log K_{sp} = −27.39,

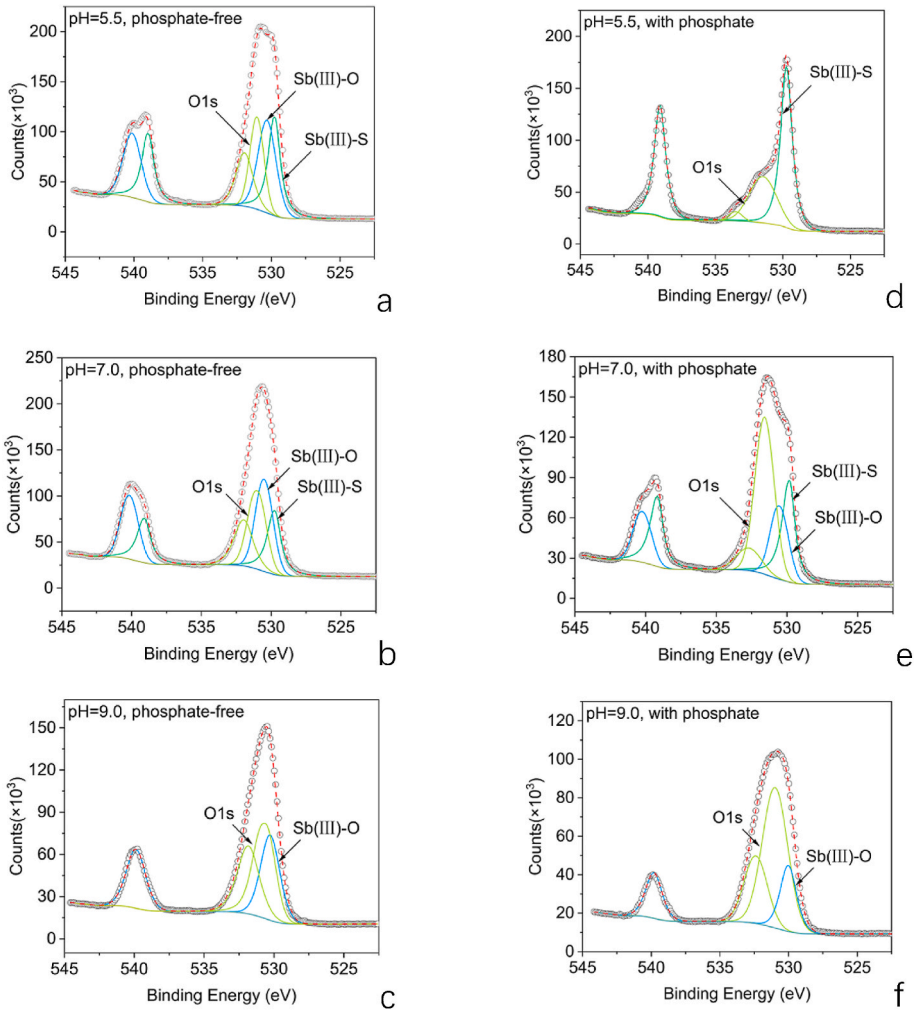

Fig. 5. XPS spectra of Sb 3d peaks for the solid phases (a, b, and c: experiments P-0 at pH 5.5, 7.0, and 9.0; d, e, and f: experiments P-95 at pH 5.5, 7.0, and 9.0).

Jong and Parry, 2003). The difference in solubility product indicates that Sb(III) can possibly outcompete Fe(II) in binding to $S(-II)_{aq}$. The competition of Sb(III) and Fe(II) for $S(-II)_{aq}$ can be described by the following equilibrium reaction between FeS and amorphous Sb_2S_3.

$$3\ FeS_{(s)} + 2\ Sb(OH)_3 + 6\ H^+ \rightleftharpoons Sb_2S_{3(s)} + 3\ Fe^{2+} + 6\ H_2O \quad \ldots\ldots\ldots \quad (1)$$

This reaction is dependent of pH. When pH decreases, FeS becomes more soluble (Wolthers et al., 2005; Han et al., 2018) and releases more S(–II) that subsequently react with Sb(III). Moreover, the stability of Sb_2S_3 can increase significantly with decreasing pH (Krupp, 1988; Spycher and Reed, 1989; Olsen et al., 2018). Similar to Sb_2S_3, the stability of As_2S_3 has also been reported to increase under acidic conditions (Wilkin and Ford, 2002; Rodriguez-Freire et al., 2014). Therefore, the precipitation of Sb_2S_3 in the interaction of Sb(III) with FeS can be enhanced at lower pH. When pH increases, FeS becomes more stable and is more difficult to dissolve. In the pH 9.0 experiments, the concentrations of Fe(II) were close to zero, indicating that FeS did not dissolve. In these experiments, FeS was initially synthesized by addition of Fe(II) and S(–II) at a molar ratio of 1:1. Although the molar ratio of Fe:S in this material could vary, Rickard et al. (2006) reported a stoichiometric composition of $Fe_{1.00\pm0.01}S$ in which this ratio was very close to 1:1. Therefore, very minor S(–II) could be expected to be available for the formation of Sb_2S_3.

The stability fields of FeS and Sb_2S_3 according to reaction (1) are shown in Fig. 6. It can be seen that the conditions of the pH 5.5 and pH 7.0 experiments were favorable for the formation of Sb_2S_3. The conditions of the pH 9.0 experiments were not shown because the concentrations of Fe(II) were close to zero. Anyway, the stability field of Sb_2S_3 at pH 9.0 was shown to be much smaller than that at pH 5.5 and pH 7.0. Consistent with the discussion above, precipitates of Sb_2S_3 were observed in the pH 5.5 and pH 7.0 experiments, but not observed in the pH 9.0 experiments.

When excess sulfide is available, Sb_2S_3 becomes less stable because it can complex with sulfide to form thioantimonite species (e.g., $Sb_2S_4^{2-}$ and $HSb_2S_4^-$) under alkaline conditions (Polack et al., 2009; Planer--Friedrich and Scheinost, 2011). In the pH 9 experiments, FeS was very stable and $S(-II)_{aq}$ was basically not available (as mentioned above) for the formation of thioantimonite species, so Sb(III) should be mainly present as $Sb(OH)_3$. This is consistent with the result of Olsen et al. (2018). They reported that, in a solution containing 3.2 mg/L $S(-II)_{aq}$, $Sb(OH)_3$ was the predominant species from pH 7.5 to 11.8 whereas $HSb_2S_4^-$ was predominant from pH 6.4 to 7.5. In the pH 5.5 and pH 7.0 experiments, partial dissolution of FeS occurred (Fig. 2b) and the concentration of the released S(–II)aq was calculated to be 10.4 and 1.2 mg/L, respectively. A comparison between these data and result of Olsen et al. (2018) indicates that, in the pH 7.0 experiments, the presence of $HSb_2S_4^-$ could be of significance. However, it seems difficult to identify the presence of thioanimonite species in the pH 5.5 experiments, because the stability of thioantimonite species is much lower at lower pH (Krupp, 1988; Olsen et al., 2018).

In aqueous environments, PO_4^{3-} has a potential to react with Fe(II) and form a precipitate of $Fe_3(PO_4)_2{\cdot}8H_2O$ (Nriagu, 1972). The formation

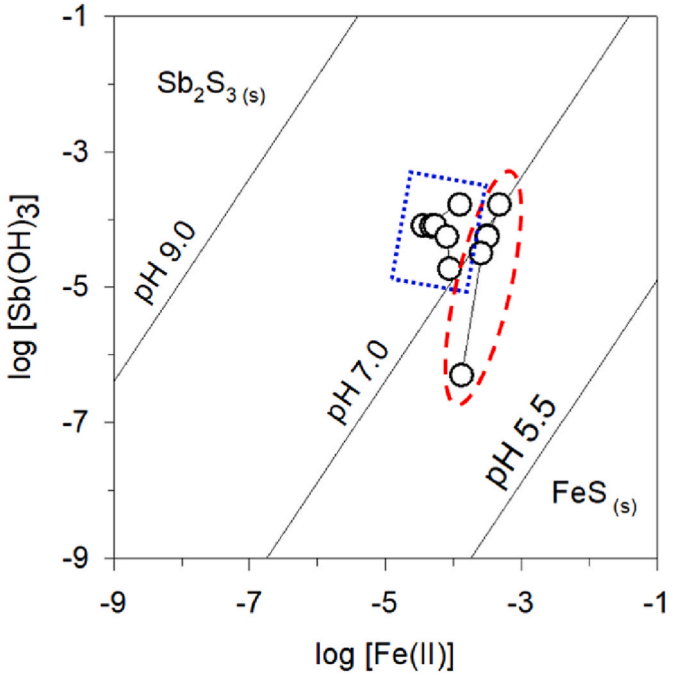

Fig. 6. Stability fields for FeS versus Sb_2S_3 (adapted from Hockmann et al., 2020). Background NaCl concentration was 0.1 M. Symbols in the elliptical and the rectangular areas indicate the conditions of pH 5.5 and pH 7.0 experiments, respectively.

of $Fe_3(PO_4)_2{\cdot}8H_2O$ has been observed in lake sediments (Fagel et al., 2005; O'Connell et al., 2015; Rothe et al., 2016) and wastewaters (Wilfert et al., 2015; Li et al., 2018). In a sulfidic system, however, it is difficult for $Fe_3(PO_4)_2{\cdot}8H_2O$ to be formed because PO_4^{3-} has a lower binding strength to Fe(II) than S(–II) (Nriagu, 1972). This can be reflected by the solubility products of FeS (Log K_{sp} = −27.39) and $Fe_3(PO_4)_2{\cdot}8H_2O$ (Log K_{sp} = −36, Nriagu, 1972). It has been suggested that high activities of Fe(II) and PO_4^{3-}, as well as low S(–II) activity, are required for the formation of vivianite in lake sediments (Fagel et al., 2005; O'Connell et al., 2015). Therefore, in the FeS + Sb(III) + PO_4^{3-} system, the formation of $Fe_3(PO_4)_2{\cdot}8H_2O$ is considered possible only when high activities of Fe(II) and PO_4^{3-} are present. The reaction is described below.

$$3\ FeS + 2\ H_2PO_4^- + 2\ H^+ + H_2O \leftrightharpoons Fe_3(PO_4)_2{\cdot}8H_2O_{(s)} + 3\ H_2S \quad \ldots\ldots \quad (2)$$

Under alkaline conditions, FeS is stable and Fe(II) released into the aqueous phase is very minor, so the formation of $Fe_3(PO_4)_2{\cdot}8H_2O$ is very difficult. Under acidic and neutral conditions, FeS can dissolve to some extent and release some Fe(II) into aqueous phase, making the formation of $Fe_3(PO_4)_2{\cdot}8H_2O$ possible when PO_4^{3-} loading is high enough. This explains why precipitates of $Fe_3(PO_4)_2{\cdot}8H_2O$ were only observed in the experiments at pH 5.5 and 7.0 with high PO_4^{3-} loadings (95 and 475 mg/L). Consistently, Schoepfer et al. (2019) reported that a higher PO_4^{3-} loading led to the formation of more vivianite at expense of FeS. The formation of $Fe_3(PO_4)_2{\cdot}8H_2O$ resulted in the release of more S(–II) and accordingly enhanced the formation of Sb_2S_3. Basically, the adsorption of Sb(III) on $Fe_3(PO_4)_2{\cdot}8H_2O$ has been very scarcely investigated. Johnson et al. (2021) reported the presence of a small amount of Sb(III) on vivianite in the interaction of Sb(V) with vivianite. As shown in Fig. 4 and Fig. S2, very little Sb(III) was detected to be bound to $Fe_3(PO_4)_2{\cdot}8H_2O$ when compared to that bound to FeS. Therefore, it is assumed that the contribution of readsorption of Sb(III) on $Fe_3(PO_4)_2{\cdot}8H_2O$ to the removal of $Sb(III)_{aq}$ was minor.

In the experiments with high PO_4^{3-} loadings, the decrease in PO_4^{3-} concentration at pH 5.5 was found to be similar to that at pH 7.0 (Fig. 2c). Consistently, in the TEM examination of the solid phases of the experiments with high PO_4^{3-} loadings, $Fe_3(PO_4)_2{\cdot}8H_2O$ was observed in the pH 5.5 sample at a similar frequency as in the pH 7.0 sample, although the dissolution of FeS at pH 5.5 was stronger than that at pH 7.0. This means that the presence of a high PO_4^{3-} loading at pH 5.5 and 7.0 resulted in a similar yield of $Fe_3(PO_4)_2{\cdot}8H_2O$. This result is suggested to be related to the pH-dependent stability of $Fe_3(PO_4)_2{\cdot}8H_2O$. With changes in pH, phosphate species transform at different pKa values and the stability of $Fe_3(PO_4)_2{\cdot}8H_2O$ can be influenced (Palansooriya et al., 2021). Li et al. (2018) reported that, although $Fe_3(PO_4)_2{\cdot}8H_2O$ was stable in the solid phase at pH 6, it was largely dissolved when the pH was lowered to 5 and was mostly soluble when the pH was further decreased to 3. Overall, the stability of $Fe_3(PO_4)_2{\cdot}8H_2O$ decreased with decreasing pH, but the concurrent stronger dissolution of FeS at lower pH could compensate for the formation of $Fe_3(PO_4)_2{\cdot}8H_2O$.

The mitigation of Sb(III) mobility in FeS-containing system by the high PO_4^{3-} loading is possibly of minor importance for most environmental systems because of the very high Sb(III) and PO_4^{3-} concentrations in the present study. In some sulfidic mine tailings sites, however, PO_4^{3-} has been increasingly utilized to stabilize metal(loid)s (Munksgaard and Lottermoser, 2013; Saavedra-Mella et al., 2019). In anoxic layers of these mine tailings, high dosages of PO_4^{3-} may encounter the presence of FeS and high concentrations of soluble metal(loid)s. For example, Ashley et al. (2003) reported Sb concentration of 55 mg L^{-1} in tailings dam seepage water in an Sb (stibnite) deposit at Hillgrove, Australia. In these settings, the effect of high loadings PO_4^{3-} on the mobility of Sb(III) can be of major importance.

4. Conclusions

In the interaction of Sb(III) with FeS, the uptake of Sb(III) could be significantly affected by PO_4^{3-}. This impact was closely related to pH and PO_4^{3-} concentration. Under slightly acidic (pH 5.5) or neutral conditions (pH 7.0), high PO_4^{3-} loadings (95 and 475 mg/L) enhanced the uptake of Sb(III) due to the formation of $Fe_3(PO_4)_2{\cdot}8H_2O$, which enhanced the dissolution of FeS and consequently the precipitation of Sb_2S_3. However, low PO_4^{3-} loadings (9.5 and 19 mg/L) did not affect the mobility of Sb(III) because $Fe_3(PO_4)_2{\cdot}8H_2O$ was not likely to be formed. Under alkaline conditions (pH 9.0), the addition of PO_4^{3-} only resulted in a minor release of Sb(III) into aqueous phase, because the interaction of Sb(III) with FeS was suggested to be dominated by the adsorption that could not be readily affected by PO_4^{3-}.

Declaration of competing interest

The authors declare that they have no known competing financial interests or personal relationships that could have appeared to influence the work reported in this paper.

Acknowledgments

This study was financially supported by the China National Key Research and Development Program (No. 2020YFC1807700) and the China National Natural Science Foundation (No. U1612442).

Appendix A. Supplementary data

Supplementary data to this article can be found online at https://doi.org/10.1016/j.apgeochem.2022.105297.

References

Amarasiriwardena, D., Wu, F., 2011. Antimony: emerging toxic contaminant in the environment. Microchem. J. 97, 1–3.

APHA, 1998. Standard Methods for the Examination of Water and Wastewater, twentieth ed. American Public Health Association/American Water Works Association, Baltimore, USA.

Ashley, P.M., Craw, D., Graham, B.P., Chappell, D.A., 2003. Environmental mobility of antimony around mesothermal stibnite deposits, New South Wales, Australia and southern New Zealand. J. Geochem. Explor. 77, 1–14.
Biswas, A., Bhattacharya, P., Mukherjee, A., Nath, B., Alexanderson, H., Kundu, A.K., Chatterjee, D., Jacks, G., 2014. Shallow hydrostratigraphy in an arsenic affected region of Bengal Basin: implication for targeting safe aquifers for drinking water supply. Sci. Total Environ. 485, 12–22.
Burton, E.D., Johnston, S.G., Bush, R.T., 2011. Microbial sulfidogenesis in ferrihydrite-rich environments: effects on iron mineralogy and arsenic mobility. Geochem. Cosmochim. Acta 75, 3072–3087.
Burton, E.D., Johnston, S.G., Kocar, B.D., 2014. Arsenic mobility during flooding of contaminated soil: the effect of microbial sulfate reduction. Environ. Sci. Technol. 48, 13660–13667.
Burton, E.D., Hockmann, K., Karimian, N., Johnston, S.G., 2019. Antimony mobility in reducing environments: the effect of microbial iron(III)-reduction and associated secondary mineralization. Geochem. Cosmochim. Acta 245, 278–289.
Dodd, J., Large, D.J., Fortey, N.J., Kemp, S., Styles, M., Wetton, P., Milodowski, A., 2003. Geochemistry and petrography of phosphorus in urban canal bed sediment. Appl. Geochem. 18, 259–267.
Fagel, N., Alleman, L.Y., Granina, L., Hatert, F., Thamo-Bozso, E., Cloots, R., Andre, L., 2005. Vivianite formation and distribution in Lake Baikal sediments. Global Planet. Change 46, 315–336.
Filella, M., Belzile, N., Chen, Y.-W., 2002a. Antimony in the environment: a review focused on natural waters I. Occurrence. Earth Sci. Rev. 57, 125–176.
Filella, M., Belzile, N., Chen, Y.-W., 2002b. Antimony in the environment: a review focused on natural waters II. Relevant solution chemistry. Earth Sci. Rev. 59, 265–285.
Filella, M., Williams, P.A., 2010. Antimony biomethylation in culture media revisited in the light of solubility and chemical speciation considerations. Environ. Toxicol. 25, 431–439.
Filella, M., Williams, P.A., 2012. Antimony interactions with heterogeneous complexants in waters, sediments and soils: a review of binding data for homologous compounds. Chem. Erde 72 (S4), 49–65.
Fu, Z., Zhang, G., Li, H., Chen, J., Liu, F., Wu, Q., 2016. Influence of reducing conditions on the release of antimony and arsenic from a tailing sediment. J. Soils Sediments 16, 2471–2481.
Gallegos, T.J., Hyun, S.P., Hayes, K.F., 2007. Spectroscopic investigation of the uptake of arsenite from solution by synthetic mackinawite. Environ. Sci. Technol. 41, 7781–7786.
Gayer, K.H., Garrett, A.B., 1952. The equilibria of antimonious oxide(rhombic) in delute solutions of hydrochloric acid and sodium hydroxide at 25 °C. J. Am. Chem. Soc. 74, 2353–2354.
Greenberg, A.E., Clesceri, L.S., Eaton, A.D., 1992. Standard Methods for the Examination of Water and Wastewater, eighteenth ed. American Public Health Association, Washington, DC, USA.
Han, Y.-S., Gallegos, T.J., Demond, A.H., Hayes, K.F., 2011. FeS-coated sand for removal of arsenic(III) under anaerobic conditions in permeable reactive barriers. Water Res. 45, 593–604.
Han, Y.-S., Seong, H.J., Chon, C.-M., Park, J.H., Nam, I.-H., Yoo, K., Ahn, J.S., 2018. Interaction of Sb(III) with iron sulfide under anoxic conditions: similarities and differences compared to As(III) interactions. Chemosphere 195, 762–770.
Han, Y.-S., M, C., Park, J.H., Min, Y., Lim, D.-H., 2020. Competitive adsorption between phosphate and arsenic in soil containing iron sulfide: XAS experiment and DFT calculation approaches. Chem. Eng. J. 397, 125426.
He, M.C., Wang, X.Q., Wu, F.C., Fu, Z.Y., 2012. Antimony pollution in China. Sci. Total Environ. 421, 41–50.
Hockmann, K., Planer-friedrich, B., Johnston, S.G., Peiffer, S., Burton, E.D., 2020. Antimony mobility in sulfidic systems: coupling with sulfide-induced iron oxide transformations. Geochem. Cosmochim. Acta 282, 276–296.
Jeong, H.Y., Lee, J.H., Hayes, K.F., 2008. Characterization of synthetic nanocrystalline mackinawite: crystal structure, particle size, and specific surface area. Geochem. Cosmochim. Acta 72, 493–505.
Johnson, C.R., Antonopoulos, D.A., Boyanov, M.I., Flynn, T.M., Koval, J.C., Kemmer, K. M., O'Loughlin, E.J., 2021. Reduction of Sb(V) by couple biotic-abiotic process under sulfidogenic conditions. Heliyon 7, e06275.
Jong, T., Parry, D.L., 2003. Removal of sulfate and heavy metals by sulfate reducing bacteria in short-term bench scale upflow anaerobic packed bed reactor runs. Water Res. 37, 3379–3389.
Kirsch, R., Scheinost, A.C., Rossberg, A., Banerjee, D., Charlet, L., 2008. Reduction of antimony by nano-particulate magnetite and mackinawite. Mineral. Mag. 72, 185–189.
Kocar, B.D., Borch, T., Fendorf, S., 2010. Arsenic repartitioning during biogenic sulfidization and transformation of ferrihydrite. Geochem. Cosmochim. Acta 74, 980–994.
Krupp, R.E., 1988. Solubility of stibnite in hydrogen-sulfide solutions, speciation, and equilibrium-constants, from 25 to 350 °C. Geochem. Cosmochim. Acta 52, 3005–3015.
Kulp, T.R., Miller, L.G., Braiotta, F., Webb, S.M., Kocar, B.D., Blum, J.S., Oremland, R.S., 2014. Microbiological reduction of Sb(V) in anoxic freshwater sediments. Environ. Sci. Technol. 48, 218–226.
Li, Y.-L., Vali, H., Yang, J., Phelps, T.J., Zhang, C.L., 2006. Reduction of iron oxides enhanced by a sulfate-reducing bacterium and biogenic H_2S. Geomicrobiol. J. 23, 103–117.
Li, R.-h., Cui, J.-L., Li, X.-D., Li, X.-y., 2018. Phosphorus removal and recovery from wastewater using Fe dosing bioreactor and co-fermentation: investigation by X-ray absorption near edge structure (XANES) spectroscopy. Environ. Sci. Technol. 52, 14119–14128.
Li, X., Reich, T., Kersten, M., Jing, C., 2019. Low-Molecular-weight organic acid complexation affects antimony(III) adsorption by granular ferric hydroxide. Environ. Sci. Technol. 53, 5221–5229.
Li, D., Zhang, G., Wang, Q., Liu, S., Ma, C., Chen, J., Liu, F., 2021. Interaction of aqueous antimony(III) with synthetic ferrous sulfide. Appl. Geochem. 128, 104957.
Liu, M., Wang, C., Guo, J., Zhang, L., 2021. Removal of phosphate from wastewater by lanthanum modified bio-ceramisite. J. Environ. Chem. Eng. 9, 106123.
Ma, C., Zhang, G., Chen, J., Wang, Q., Liu, F., 2020. Transfer of FeS-bound arsenic into pyrite during the transformation of amorphous FeS to pyrite. Appl. Geochem. 119, 104645.
Mane, R.S., Lokhande, C.D., 2003. Thickness-dependent properties of chemically deposited Sb_2S_3 thin films. Mater. Chem. Phys. 82, 347–354.
Munksgaard, N.C., Lottermoser, B.G., 2013. Phosphate amendment of metalliferous tailings, Cannington Ag-Pb-Zn mine, Australia: implications for the capping of tailings storage facilities. Environ. Earth Sci. 68, 33–44.
Neidhardt, H., Schoeckle, D., Schleinitz, A., Eiche, E., Berner, Z., Tram, P.T.K., Lan, V.M., Viet, P.H., Biswas, A., Majumder, S., Chatterjee, D., Oelmann, Y., Berg, M., 2018. Biogeochemical phosphorus cycling in groundwater ecosystems – insights from South and Southeast Asian floodplain and delta aquifers. Sci. Total Environ. 644, 1357–1370.
Neidhardt, H., Rudischer, S., Eiche, E., Schneider, M., Stopelli, E., Duyen, V.T., Trang, P. T.K., Viet, P.H., Newmann, T., Berg, M., 2021. Phosphate immobilisation dynamics and interaction with arsenic sorption at redox transition zones in floodplain aquifers: insights from the Red River Delta, Vietnam. J. Hazard Mater. 411, 125128.
Niazi, N.K., Burton, E.D., 2016. Arsenic sorption to nanoparticulate mackinawite (FeS): an examination of phosphate competition. Environ. Pollut. 218, 111–117.
Nriagu, J.O., 1972. Stability of vivianite and ion-pair formation in the system $Fe_3(PO_4)_2$ - H_3PO_4 - H_2O. Geochem. Cosmochim. Acta 36, 459–470.
O'Connell, D.W., Jensen, M.M., Jakobsen, R., Thamdrup, B., Andersen, T.J., Kovacs, A., Hansen, H.C.B., 2015. Vivianite formation and its role in phosphorus retention in Lake Ørn, Denmark. Chem. Geol. 409, 42–53.
Olsen, N.J., Mountain, B.W., Seward, T.M., 2018. Antimony(III) sulfide complexes in aqueous solutions at 30°C: a solubility and XAS study. Chem. Geol. 476, 233–247.
Palansooriya, K.N., Kim, S., Igalavithana, A.D., Hashimoto, Y., Choi, Y.E., Mukhopadhyay, R., Sarkar, B., Ok, Y.S., 2021. Fe(III) loaded chitosan-biochar composite fibers for the removal of phosphate from water. J. Hazard Mater. 415, 125464.
Park, J.-H., Kim, S.-J., Ahn, J.S., Lim, D.-H., Han, Y.-S., 2018. Mobility of multiple heavy metalloids in contaminated soil under various redox conditions: effects of iron sulfide presence and phosphate competition. Chemosphere 197, 344–352.
Planer-Friedrich, B., Scheinost, A.C., 2011. Formation and structural characterization of thioantimony species and their natural occurrence in geothermal waters. Environ. Sci. Technol. 45, 6855–6863.
Podgorski, J., Berg, M., 2020. Global threat of arsenic in groundwater. Science 368, 845–850.
Polack, R., Chen, Y.-W., Belzile, N., 2009. Behaviour of Sb(V) in the presence of dissolved sulfide under controlled anoxic aqueous conditions. Chem. Geol. 262, 179–185.
Rathi, B., Neidhardt, H., Berg, M., Siade, A., Prommer, H., 2017. Processes governing arsenic retardation on Pleistocene sediments: adsorption experiments and model based analysis. Water Resour. Res. 53, 4344–4360.
Rickard, D., Griffith, A., Oldroyd, A., Butler, I.B., Lopez-Capel, E., Manning, D.A.C., Apperley, D.C., 2006. The composition of nanoparticulate mackinawite, tetragonal iron(II) monosulfide. Chem. Geol. 235, 286–298.
Rodriguez-Freire, L., Sierra-Alvarez, R., Root, R., Chorover, J., Field, J., 2014. Biomineralization of arsenate to arsenic sulfides is greatly enhanced at mildly acidic conditions. Water Res. 66, 242–253.
Rothe, M., Kleeberg, A., Hupfer, M., 2016. The occurrence, identification and environmental relevance of vivianite in waterlogged soils and aquatic sediments. Earth Sci. Rev. 158, 51–64.
Saavedra-Mella, F., Liu, Y., Southam, G., Huang, L., 2019. Phosphate treatment alleviated acute phytotoxicity of heavy metals in sulfidic Pb-Zn mine tailings. Environ. Pollut. 250, 676–685.
Schoepfer, V., Burton, E.D., Johnston, S.G., Kraal, P., 2019. Phosphate loading alters schwertmannite transformation rates and pathways during microbial reduction. Sci. Total Environ. 657, 770–780.
Spycher, N.F., Reed, M.H., 1989. As(III) and Sb(III) sulfide complexes: an evaluation of stoichiometry and stability from existing experimental data. Geochem. Cosmochim. Acta 53, 2185–2194.
Ungureanu, G., Santos, S., Boaventura, R., Botelho, C., 2015. Arsenic and antimony in water and wastewater: overview of removal techniques with special reference to latest advances in adsorption. J. Environ. Manag. 151, 326–342.
von Bromssen, M., Haller Larsson, S., Bhattacharya, P., Hasan, M.A., Ahmed, K.M., Jakariya, M., Sikder, M.A., Sracek, O., Biven, A., Dousova, B., Patriarca, C., Thunvik, R., Jacks, G., 2008. Geochemical characterisation of shallow aquifer sediments of Matlab Upazila, Southeastern Bangladesh - implications for targeting low-As aquifers. J. Contam. Hydrol. 99, 137–149.
Watson, J.H.P., Ellwood, D.C., Deng, Q., Mikhalovsky, S., Hayter, C.E., Evans, J., 1995. Heavy metal adsorption on bacterially produced FeS. Miner. Eng. 8 (10), 1097–1108.
Wilkin, R., Ford, R., 2002. Use of hydrochloric acid for determining solid-phase arsenic partitioning in sulfidic system. Environ. Sci. Technol. 36, 4921–4927.
Wilson, S.C., Lockwood, P.V., Ashley, P.M., Tighe, M., 2010. The chemistry and behaviour of antimony in the soil environment with comparisons to arsenic: a critical review. Environ. Pollut. 158, 1169–1181.

Wilfert, P., Kumar, P.S., Korving, L., Witkamp, G.-J., Van Loosdrecht, M.C.M., 2015. The relevance of phosphorus and iron chemistry to the recovery of phosphorus from wastewater: a review. Environ. Sci. Technol. 49, 9400–9414.
Wolthers, M., van der Gaast, S.J., Rickard, D., 2003. The structure of disordered mackinawite. Am. Mineral. 88, 2007–2015.
Wolthers, M., Charlet, L., van der Weijden, C.H., van der Linde, P.R., Ricard, D., 2005. Arsenic mobility in the ambient sulfidic environment; sorption of arsenic(V) and arsenic(III) onto disordered mackinawite. Geochem. Cosmochim. Acta 69, 3483–3492.